

RESEARCH REPORTS

Biological

H. Cao¹, J. Wang¹, X. Li¹, S. Florez¹, Z. Huang¹,
S.R. Venugopalan¹, S. Elangovan², Z. Skobe²,
H.C. Margolis², J.F. Martin¹, and B.A. Amendt^{1*}

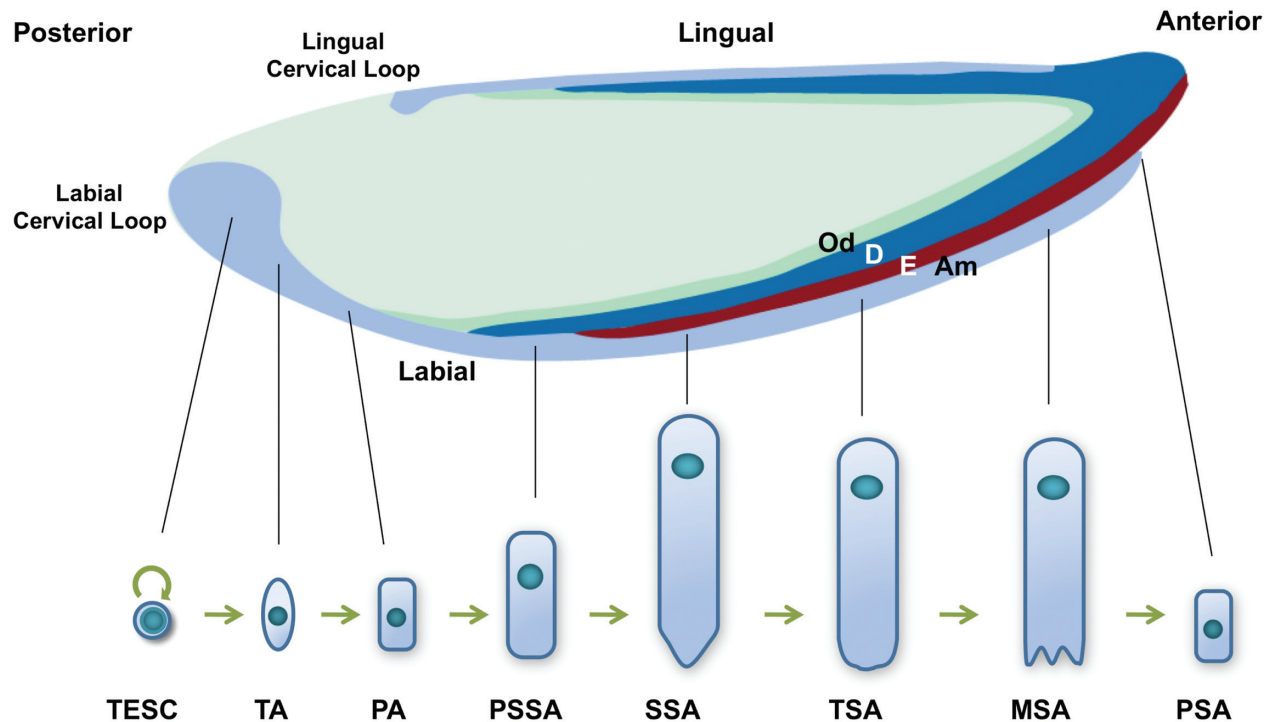
¹Institute of Biosciences and Technology, Texas A&M Health Science Center, 2121 W. Holcombe Boulevard, Houston, TX 77030, USA; and

²Department of Biominerization, The Forsyth Institute, Boston, MA, USA;

*corresponding authors, bamendt@ibt.tamhsc.edu

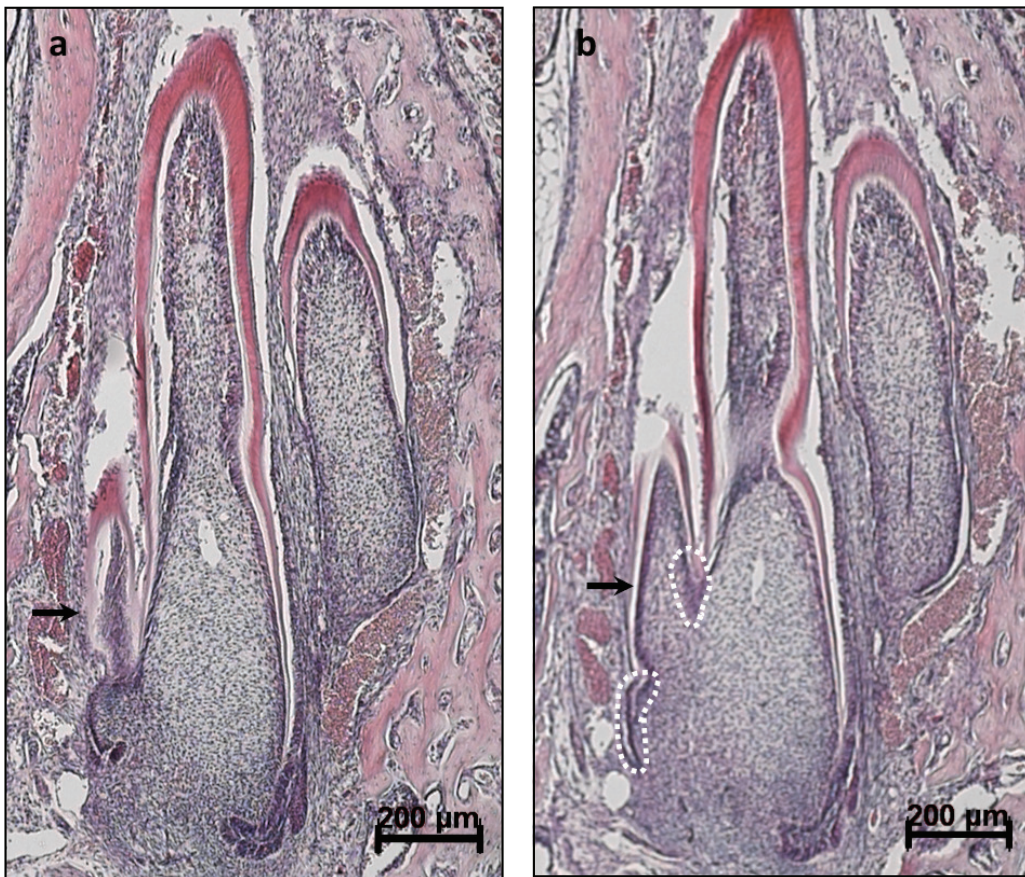
J Dent Res 89(8):779-784, 2010

APPENDIX

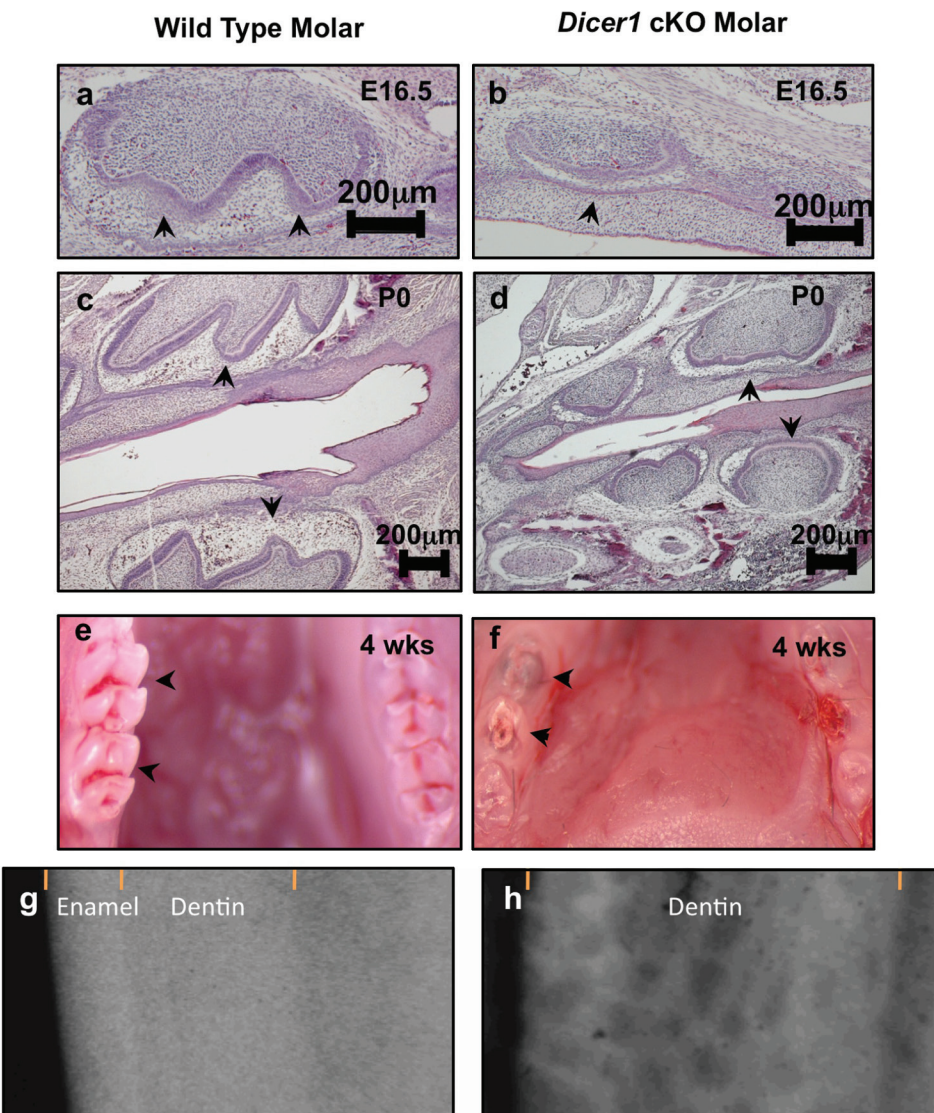


TESC: Tooth Epithelial Stem Cell, TA: Transit Amplify cell, PA: Pre-Ameloblast cell,
PSSA:Pre-Secretory Stage Ameloblast, SSA: Secretory Stage Ameloblast,
TSA: Transit Stage Ameloblast, MSA: Mature Stage Ameloblast, PSA: Protective Stage Ameloblast

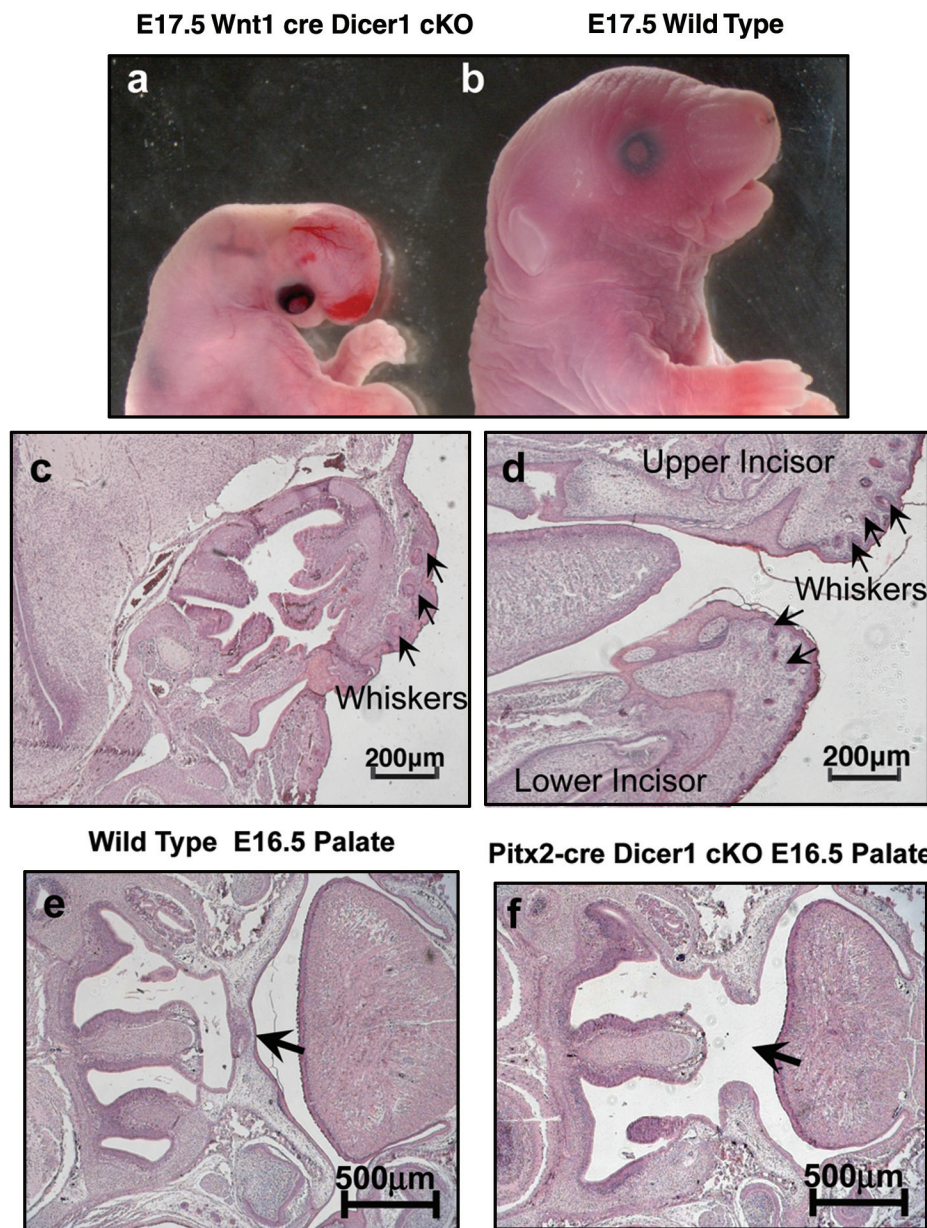
Appendix Figure 1. Schematic diagram of an adult incisor. Enamel (shown in red) and dentin (blue) are produced by ameloblasts and odontoblasts, respectively. Different from dentin, which is present at lingual and labial sides, enamel is present only on the labial side. There are different stages of cell differentiation present on the labial side: TESC, tooth epithelial stem cells; TA, transit-amplifying cells; PA, pre-ameloblast cells; PSSA, pre-secretory-stage ameloblasts; SSA, secretory-stage ameloblasts; TSA, transit-stage ameloblasts; MSA, mature-stage ameloblasts; PSA, protective-stage ameloblasts. The post-mitotic cells are from stages PSSA to PSA.



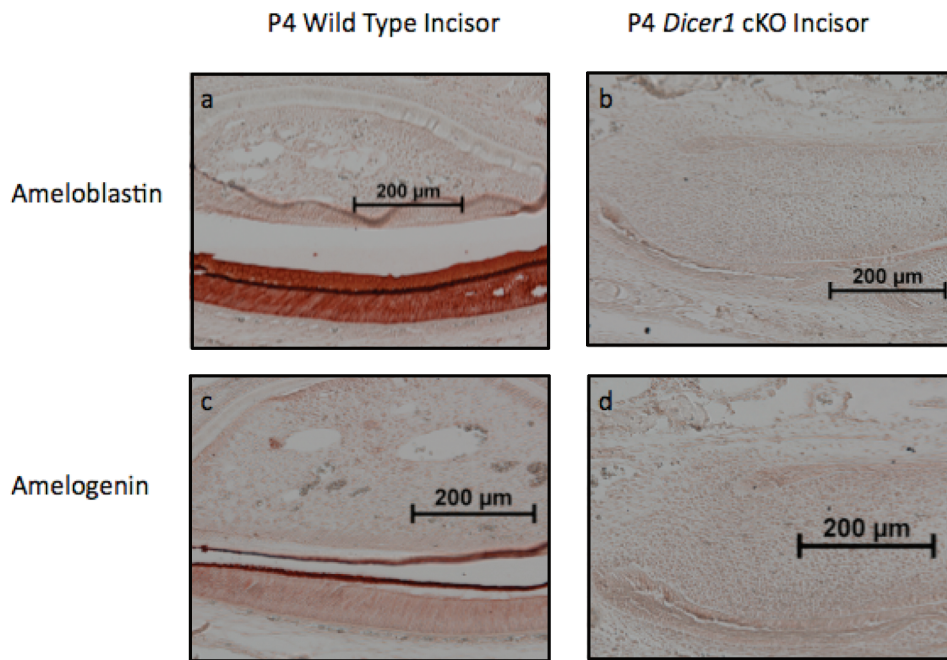
Appendix Figure 2. Branching of *Pitx2-Cre/Dicer1* cKO incisor. **(a,b)** Histology of 2 close sections of two-week-old *Pitx2-Cre/Dicer1* cKO heads. Note the extra incisor branching from the posterior end of one incisor (arrows). The potential new cervical loops are outlined by the white dotted line.



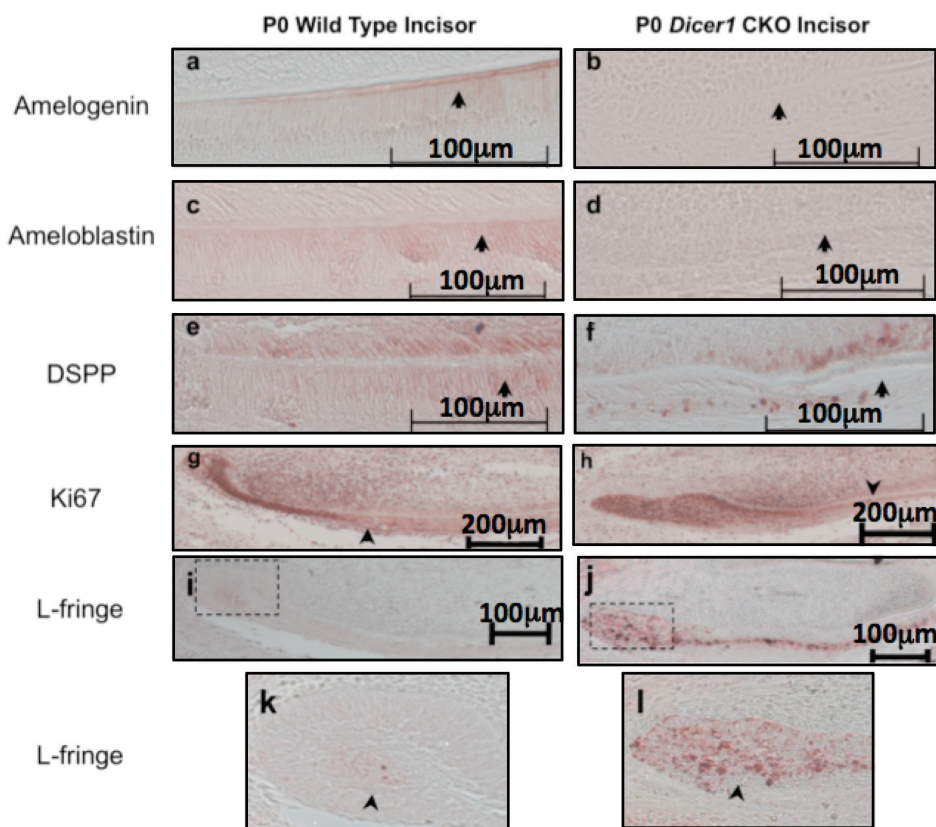
Appendix Figure 3. Severe molar defects in *Pitx2-Cre/Dicer1 cKO*. **(a,b)** At E16.5, the molars are abnormally formed in the *Pitx2-Cre/Dicer1 cKO* mouse. **(c,d)** In P0 *Pitx2-Cre/Dicer1 cKO*, molar cusp formation was defective (arrows). Sagittal sections of newborn (P0) wild-type and *Pitx2-Cre/Dicer1 cKO* heads. In the *Dicer1 cKO*, molar morphology was severely disrupted, with no cusp formation and relatively small molar tooth germs (arrows). **(e,f)** In one-month-old mutant mice, the erupted molars were small and lacked the characteristic cusps of the WT mice. **(g,h)** X-ray microradiographs of three-month-old WT and *Dicer1 cKO* incisors. *Dicer1 cKO* have no enamel. Dentin deposition was also affected.



Appendix Figure 4. Severe craniofacial defects in *Wnt1-Cre/Dicer1* and *Pitx2-Cre/Dicer1* cKO. **(a,b)** At E17.5, *Wnt1-Cre/Dicer1* cKO had severe craniofacial defects. Mouth and nose structures are missing. In contrast, the brain is relatively expanded. **(c,d)** Sagittal sections of E17.5 *Wnt1-Cre/Dicer1* cKO and WT embryos, respectively. Upper jaw, lower jaw, tongue, and other structures are missing in the mutant mouse head. The major part of the head is brain tissue. Whiskers (arrows) are clearly formed in *Wnt1-Cre/Dicer1* cKO. **(e,f)** Coronal sections of E16.5 wild-type and *Pitx2-Cre/Dicer1* cKO heads. Cleft palate in *Pitx2-Cre/Dicer1* cKO (arrows).



Appendix Figure 5. Ameloblast differentiation defect in P4 incisor. (a-d) Ameloblast differentiation markers observed by immunohistochemistry of P4 wild-type and *Pitx2-Cre/Dicer1* cKO lower incisors. Amelogenin and Ameloblastin. Note the dramatic decrease of amelogenin and ameloblastin in *Pitx2-Cre/Dicer1* cKO compared with WT.



Appendix Figure 6. Ameloblast differentiation is repressed in the *Pitx2-Cre/Dicer1* cKO. (g-f) Higher-magnification pictures of the boxed region of Fig. 3 in the main article. (g,h) Ki67, a cell proliferation marker observed by immunohistochemistry of newborn (P0) wild-type and *Pitx2-Cre/Dicer1* cKO lower incisors. Epithelial stem cells, transit-amplifying cells, and pre-ameloblast cells are proliferative (Ki67-positive). After cells enter terminal differentiation, they become post-mitotic cells (arrows). In the *Pitx2-Cre/Dicer1* cKO, a similar pattern of Ki67 staining was observed compared with that in WT incisors. (i-l) Lunatic Fringe (L-fringe), an undifferentiated cell marker, was observed by immunohistochemistry of newborn (P0) lower incisors. Dramatic up-regulation of L-fringe in the *Pitx2-Cre/Dicer1* cKO incisor (arrows). Lunatic Fringe is present inside and outside of the cervical loop region in *Pitx2-Cre/Dicer1* cKO incisor.

Appendix Table. MicroRNA Expression Profile of PO Incisor and Molar*

PO Incisor miRNAs	PO Molar				
	Signal Intensity	Frequency	miRNAs	Signal Intensity	Frequency
mmu-miR-709	57,358.77	4.60%	mmu-miR-709	49,495.29	4.05%
mmu-miR-199a-3p	46,521.57	3.73%	mmu-let-7a	44,593.04	3.65%
mmu-let-7a	45,376.98	3.64%	mmu-let-7f	41,739.87	3.41%
mmu-let-7f	41,080.46	3.29%	mmu-miR-203	41,524.82	3.40%
mmu-miR-26a	40,591.04	3.26%	mmu-let-7d	39,765.27	3.25%
mmu-miR-214	38,074.63	3.05%	mmu-let-7c	39,663.94	3.24%
mmu-let-7d	37,884.85	3.04%	mmu-miR-26a	36,084.15	2.95%
mmu-let-7c	36,689.75	2.94%	mmu-let-7b	35,016.12	2.86%
mmu-let-7i	33,298.43	2.67%	mmu-miR-23b	34,907.85	2.86%
mmu-miR-23b	31,446.16	2.52%	mmu-miR-125b-5p	33,408.51	2.73%
mmu-miR-23a	30,289.37	2.43%	mmu-miR-23a	32,470.91	2.66%
mmu-let-7b	30,241.70	2.43%	mmu-miR-199a-3p	30,565.13	2.50%
mmu-miR-125b-5p	29,975.41	2.40%	mmu-let-7e	30,472.45	2.49%
mmu-let-7g	28,748.68	2.31%	mmu-miR-214	28,147.74	2.30%
mmu-let-7e	27,461.71	2.20%	mmu-let-7i	25,645.36	2.10%
mmu-miR-762	25,908.00	2.08%	mmu-let-7g	23,732.31	1.94%
mmu-miR-335-5p	23,711.76	1.90%	mmu-miR-205	23,522.73	1.92%
mmu-miR-26b	21,780.71	1.75%	mmu-miR-26b	22,297.69	1.82%
mmu-miR-126-3p	20,782.32	1.67%	mmu-miR-762	18,533.31	1.52%
mmu-miR-21	18,968.70	1.52%	mmu-miR-200c	18,517.64	1.51%
mmu-miR-181b	18,122.74	1.45%	mmu-miR-200b	16,512.10	1.35%
mmu-miR-690	17,372.58	1.39%	mmu-miR-125a-5p	15,618.24	1.28%
mmu-miR-148a	17,159.70	1.38%	mmu-miR-15b	15,537.65	1.27%
mmu-miR-16	16,813.83	1.35%	mmu-miR-30c	15,387.77	1.26%
mmu-miR-1	16,554.61	1.33%	mmu-miR-16	15,017.26	1.23%
mmu-miR-206	16,396.95	1.32%	mmu-miR-92a	14,976.83	1.23%
mmu-miR-181a	16,237.82	1.30%	mmu-miR-335-5p	14,934.37	1.22%
mmu-miR-152	15,975.90	1.28%	mmu-miR-30b	13,941.05	1.14%
mmu-miR-27b	14,230.38	1.14%	mmu-miR-206	13,421.63	1.10%
mmu-miR-125a-5p	13,947.77	1.12%	mmu-miR-181b	13,171.20	1.08%
mmu-miR-181d	13,913.29	1.12%	mmu-miR-27b	12,949.16	1.06%
mmu-miR-30b	13,644.05	1.09%	mmu-miR-126-3p	12,279.08	1.00%
mmu-miR-705	13,238.12	1.06%	mmu-miR-21	11,979.47	0.98%
mmu-miR-30c	13,072.94	1.05%	mmu-miR-1	11,780.26	0.96%
mmu-miR-1224	12,536.62	1.01%	mmu-miR-218	11,731.64	0.96%
mmu-miR-24	12,252.04	0.98%	mmu-miR-690	11,611.42	0.95%
mmu-miR-218	12,011.71	0.96%	mmu-miR-25	11,280.79	0.92%
mmu-miR-27a	11,459.57	0.92%	mmu-miR-98	11,208.67	0.92%
mmu-miR-25	11,339.22	0.91%	mmu-miR-181d	11,154.42	0.91%
mmu-miR-92a	10,610.63	0.85%	mmu-miR-183	9,796.57	0.80%
mmu-miR-15b	10,040.89	0.81%	mmu-miR-24	9,478.12	0.78%
mmu-miR-20a	7,429.15	0.60%	mmu-miR-181a	8,884.15	0.73%
mmu-miR-140*	7,375.85	0.59%	mmu-miR-705	8,748.92	0.72%
mmu-miR-320	7,027.72	0.56%	mmu-miR-27a	8,405.48	0.69%
mmu-miR-98	6,994.34	0.56%	mmu-miR-320	7,883.54	0.64%
mmu-miR-145	6,692.53	0.54%	mmu-miR-20a	7,469.63	0.61%
mmu-miR-191	6,405.98	0.51%	mmu-miR-92b	7,416.57	0.61%
mmu-miR-199a-5p	6,175.63	0.50%	mmu-miR-17	6,696.92	0.55%
mmu-miR-574-5p	6,143.13	0.49%	mmu-miR-191	6,690.83	0.55%
mmu-miR-379	6,005.92	0.48%	mmu-miR-152	6,533.26	0.53%
mmu-miR-351	5,973.97	0.48%	mmu-miR-1224	6,506.25	0.53%
mmu-miR-17	5,799.50	0.47%	mmu-miR-574-5p	6,378.28	0.52%
mmu-miR-127	5,609.27	0.45%	mmu-miR-31	6,306.61	0.52%
mmu-miR-689	5,480.17	0.44%	mmu-miR-182	6,163.93	0.50%
mmu-miR-455	5,234.79	0.42%	mmu-miR-145	6,133.06	0.50%
mmu-miR-205	5,036.10	0.40%	mmu-miR-361	5,277.36	0.43%
mmu-miR-99b	4,995.07	0.40%	mmu-miR-379	5,214.85	0.43%
mmu-miR-151-5p	4,930.30	0.40%	mmu-miR-127	5,037.86	0.41%
mmu-miR-483	4,881.35	0.39%	mmu-miR-805	4,966.63	0.41%
mmu-miR-195	4,792.30	0.38%	mmu-miR-455	4,945.18	0.40%
mmu-miR-92b	4,460.00	0.36%	mmu-miR-99a	4,868.79	0.40%
mmu-miR-30d	4,270.40	0.34%	mmu-miR-429	4,593.30	0.38%

(continued)

Appendix Table. (continued)

PO Incisor miRNAs	PO Molar				
	Signal Intensity	Frequency	miRNAs	Signal Intensity	Frequency
mmu-miR-361	4,038.43	0.32%	mmu-miR-103	4,487.75	0.37%
mmu-miR-199b*	3,993.12	0.32%	mmu-miR-151-5p	4,463.77	0.37%
mmu-miR-143	3,752.78	0.30%	mmu-miR-100	4,425.64	0.36%
mmu-miR-103	3,711.00	0.30%	mmu-miR-148a	4,316.10	0.35%
mmu-miR-30a	3,670.66	0.29%	mmu-miR-99b	4,247.24	0.35%
mmu-miR-1187	3,642.45	0.29%	mmu-miR-107	4,201.16	0.34%
mmu-miR-99a	3,595.25	0.29%	mmu-miR-199a-5p	4,011.84	0.33%
mmu-miR-200c	3,573.82	0.29%	mmu-miR-195	3,977.25	0.33%
mmu-miR-322	3,540.56	0.28%	mmu-miR-1187	3,909.27	0.32%
mmu-miR-720	3,529.03	0.28%	mmu-miR-434-3p	3,699.96	0.30%
mmu-miR-100	3,515.71	0.28%	mmu-miR-720	3,584.30	0.29%
mmu-miR-107	3,421.59	0.27%	mmu-miR-106a	3,411.52	0.28%
mmu-miR-434-3p	3,401.53	0.27%	mmu-miR-20b	3,233.92	0.26%
mmu-miR-322*	3,327.74	0.27%	mmu-miR-451	3,211.40	0.26%
mmu-miR-133a	3,092.98	0.25%	mmu-miR-30d	3,141.88	0.26%
mmu-miR-20b	2,986.82	0.24%	mmu-miR-1196	2,927.01	0.24%
mmu-miR-450a-5p	2,984.34	0.24%	mmu-miR-30a	2,810.79	0.23%
mmu-miR-133b	2,964.65	0.24%	mmu-miR-130a	2,802.35	0.23%
mmu-miR-29a	2,597.96	0.21%	mmu-miR-199b*	2,755.91	0.23%
mmu-miR-1196	2,574.84	0.21%	mmu-miR-382	2,701.42	0.22%
mmu-miR-106a	2,487.67	0.20%	mmu-miR-351	2,679.63	0.22%
mmu-miR-382	2,459.19	0.20%	mmu-miR-106b	2,445.75	0.20%
mmu-miR-106b	2,396.09	0.19%	mmu-miR-93	2,344.24	0.19%
mmu-miR-451	2,257.03	0.18%	mmu-miR-423-5p	2,203.67	0.18%
mmu-miR-200b	2,248.28	0.18%	mmu-miR-140*	2,125.19	0.17%
mmu-miR-15a	2,238.54	0.18%	mmu-miR-674	2,087.04	0.17%
mmu-miR-181c	2,210.09	0.18%	mmu-miR-143	1,928.74	0.16%
mmu-miR-423-5p	2,151.57	0.17%	mmu-miR-342-3p	1,877.78	0.15%
mmu-miR-411*	2,086.59	0.17%	mmu-miR-1195	1,854.08	0.15%
mmu-miR-203	1,958.50	0.16%	mmu-miR-322*	1,715.93	0.14%
mmu-miR-93	1,952.39	0.16%	mmu-miR-374	1,680.16	0.14%
mmu-miR-674	1,885.90	0.15%	mmu-miR-483	1,597.60	0.13%
mmu-miR-805	1,885.05	0.15%	mmu-miR-433	1,574.93	0.13%
mmu-miR-130a	1,848.24	0.15%	mmu-miR-411*	1,557.86	0.13%
mmu-miR-495	1,811.41	0.15%	mmu-miR-15a	1,498.46	0.12%
mmu-miR-342-3p	1,762.59	0.14%	mmu-miR-19b	1,439.32	0.12%
mmu-miR-574-3p	1,705.37	0.14%	mmu-miR-322	1,393.30	0.11%
mmu-miR-378	1,704.47	0.14%	mmu-miR-676	1,369.82	0.11%
mmu-miR-467f	1,500.58	0.12%	mmu-miR-689	1,367.57	0.11%
mmu-miR-128	1,497.00	0.12%	mmu-miR-181c	1,285.33	0.11%
mmu-miR-433	1,464.25	0.12%	mmu-miR-128	1,271.65	0.10%
mmu-miR-329	1,440.03	0.12%	mmu-miR-329	1,236.64	0.10%
mmu-miR-223	1,349.03	0.11%	mmu-miR-200a	1,225.74	0.10%
mmu-miR-183	1,342.78	0.11%	mmu-miR-495	1,216.89	0.10%
mmu-miR-19b	1,261.89	0.10%	mmu-miR-134	1,191.72	0.10%
mmu-miR-466f-3p	1,245.63	0.10%	mmu-miR-133a	1,145.31	0.09%
mmu-miR-30e	1,133.69	0.09%	mmu-miR-133b	1,122.11	0.09%
mmu-miR-185	1,132.73	0.09%	mmu-miR-671-5p	1,053.35	0.09%
mmu-miR-182	1,087.28	0.09%	mmu-miR-151-3p	1,043.82	0.09%
mmu-miR-299*	1,053.09	0.08%	mmu-miR-376b	1,024.15	0.08%
mmu-miR-466i	1,023.06	0.08%	mmu-miR-541	975.77	0.08%
mmu-miR-151-3p	1,020.94	0.08%	mmu-miR-340-5p	947.00	0.08%
mmu-miR-676	979.76	0.08%	mmu-miR-574-3p	946.85	0.08%
mmu-miR-31	932.54	0.07%	mmu-miR-30e	912.85	0.07%
mmu-miR-376b	911.74	0.07%	mmu-miR-299*	896.74	0.07%
mmu-miR-374	883.61	0.07%	mmu-miR-130b	877.64	0.07%
mmu-miR-487b	844.41	0.07%	mmu-miR-185	872.77	0.07%
mmu-miR-671-5p	802.21	0.06%	mmu-miR-378	865.40	0.07%
mmu-miR-134	788.30	0.06%	mmu-miR-450a-5p	841.83	0.07%
mmu-miR-1195	776.10	0.06%	mmu-miR-708	829.82	0.07%
mmu-miR-340-5p	766.99	0.06%	mmu-miR-467f	805.81	0.07%

* Frequency: the percentages of individual microRNA signal intensity among total microRNA signal intensities.